3. Method for estimating pCO_2s

3.1. Correction for long-term trends

Since the 1960s, pCO_2s has been increasing in response to increasing CO_2 partial pressure in air (pCO_2a) (Inoue et al., 1999; Inoue and Ishii, 2005; Takahashi et al., 2009b). In order to develop a method to estimate pCO_2s by multiple regression, it is necessary to take into account these long-term trends.

In the subtropical North Pacific (excluding the southeastern portion; area 'F' in Fig. 1) and in the equatorial region where pCO_2s has been regularly observed, pCO_2s data are available with dense coverage in both space and time. Here, the long-term trends of pCO_2s can be evaluated by including the time of the observation as one of the terms in the multiple regression analysis.

In the subarctic and the southeastern subtropical North Pacific, the number of pCO_2s observations has been increasing recently, but in the past the data were few. In the South Pacific data are particularly sparse. Therefore, including the time of observations in the regression analysis does not properly determine long-term trends. Here, we investigated long-term trends of CO_2 concentrations in surface seawater (xCO_2s) in each 1° zonal band in these regions by selecting the areas and seasons for which there were sufficient data (Fig. 2a [lower] and 2b). We determined the latitudinal distributions of xCO_2s since 1969 and the latitudinal variation in the annual rate of increase of xCO_2s (Fig. 2a [upper]).

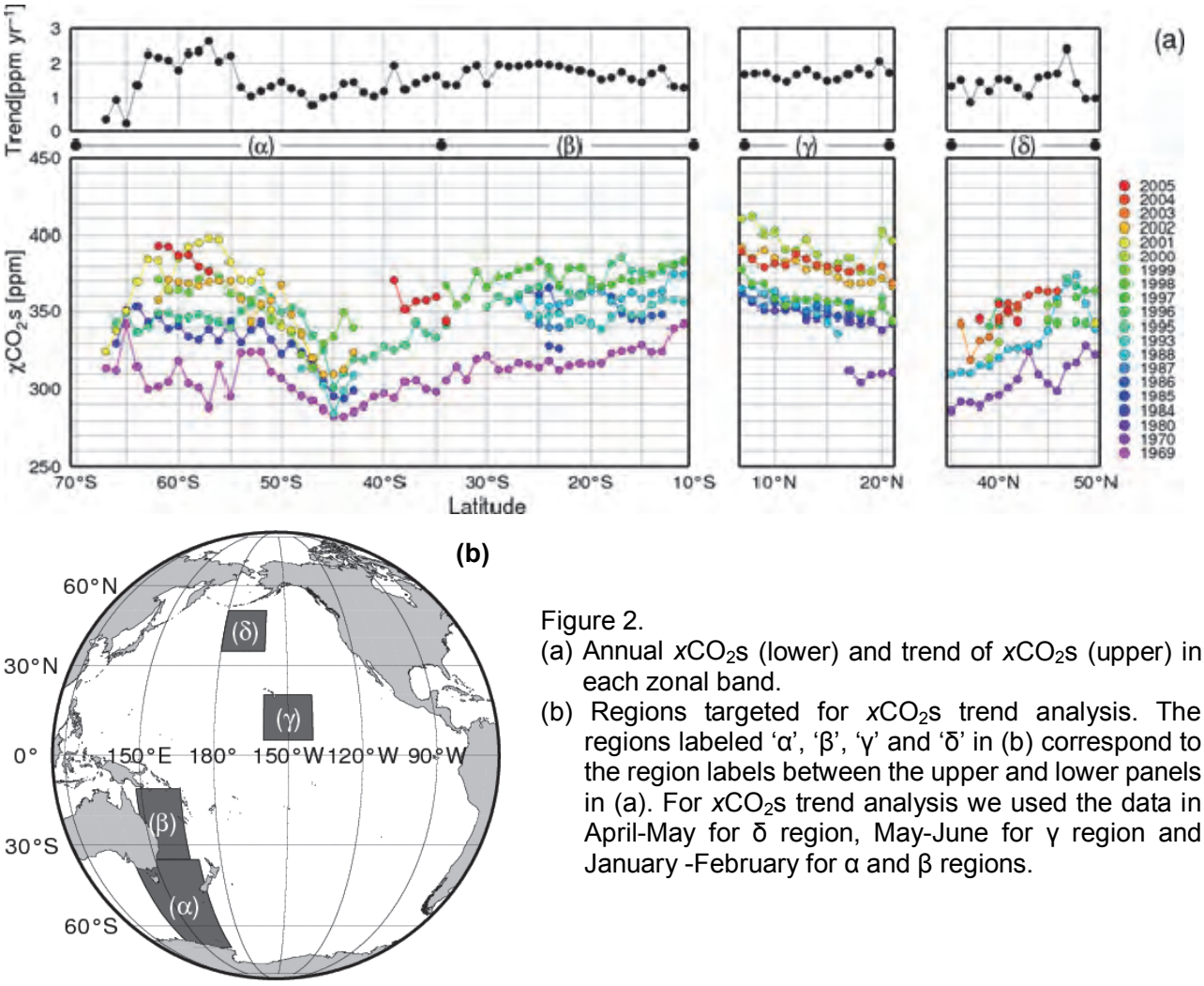

Figure 2.
(a) Annual xCO_2s (lower) and trend of xCO_2s (upper) in each zonal band.
(b) Regions targeted for xCO_2s trend analysis. The regions labeled 'α', 'β', 'γ' and 'δ' in (b) correspond to the region labels between the upper and lower panels in (a). For xCO_2s trend analysis we used the data in April-May for δ region, May-June for γ region and January -February for α and β regions.

In the subarctic North Pacific (region δ in Fig. 2b) the rates of increase range from 0.9 to 2.4 ppm yr^{-1} (average ± SD, 1.4 ± 0.4 ppm yr^{-1}). In the subtropical region (β) and (γ), the rates of increase are fairly constant with small variation; the average in both of these subtropical regions is 1.7 ± 0.2 ppm yr^{-1}. In the subantarctic South Pacific (α), the rate of increase varies from north to south. Between the subtropical front (55°S) and the subantarctic front (63°S), the rates exceed 2.0 ppm yr^{-1}. At lower latitudes (north of 55°S), the rates are 1.0 to 1.5 ppm yr^{-1}, and at higher latitudes (south of 63°S) the rates are very low. This characteristic distribution in the subantarctic South Pacific was also reported by Inoue and Ishii (2005). The average rates in this study are 1.3 ± 0.3 ppm yr^{-1} (35°S–54°S) and 2.2 ± 0.2 ppm yr^{-1} (55°S–63°S). We prepared multiple regression equations for these data-sparse regions by using the available data corrected to the year 2000 by the respective average rates of change.

3.2. Empirical method for estimating CO_2 concentration in surface seawater.

We generated acceptable empirical equations for estimating xCO_2s in each region by performing multiple regression analysis based on the relationships between SST, SSS and xCO_2s in each region (Fig. 3). Because xCO_2s varies primarily because of the thermodynamic effect from changes in temperature and salinity, we examined relationships between SSS and xCO_2s by using CO_2 data normalized to 10°C (n-xCO_2s) by using an empirical equation of Takahashi et al. (1993).

3.2.1. The subtropical region

We found a positive linear relationship between SST and xCO_2s in the subtropical region. This relationship results from the thermodynamic effect of temperature, which plays a dominant role in the variation of xCO_2s because of the shallow mixed layer and scarce nutrients (Murata et al., 1996; Takahashi et al., 2002; Park et al., 2010). Higher xCO_2s is observed in seasons with higher SST and lower xCO_2s in seasons with lower SST.

An exception is found off the coast of Peru where upwelling occurs. Coastal upwelling supplies inorganic carbon, causing higher xCO_2s in austral winter and spring. Thus the region off Peru becomes a source of atmospheric CO_2 (Friederich et al., 2008).

3.2.1.a. The North Pacific (NP/T)

In the western subtropical region (west of 160°W), there are robust linear relationships between SST and xCO_2s (red oval in Fig. 3b). xCO_2s can be estimated with small uncertainty by a linear regression with SST as reported by Murata et al. (1996). JMA observes xCO_2s along 137°E and 165°E each season as part of operations from on board the research vessels *Ryofu-Maru* and *Keifu-Maru*. Linear regression equations can be determined annually for each 1° (latitude) × 1° (longitude) grid by using these data.

In the eastern subtropical region (east of 160°W), the meridional SSS maximum is observed along about 20°N (Fig. 1). There is a negative linear relationship between n-xCO_2s and SSS north of the salinity maximum (blue oval in Fig. 3g) and a positive linear relationship south of the maximum (green oval in Fig. 3g). For this reason, we separated the northern region from the southern by the salinity maximum in the eastern subtropical North Pacific, and determined multiple regression equations with SST, SSS and year for

each region as

$$xCO_2s = 400.75 + 9.92 \cdot T_{25} - 21.26 \cdot S_{35} + 1.14 \cdot Yr_{2000} \quad (\pm \text{SE}, \pm 14.5) \qquad (1)$$

for Region E (northeastern subtropical region; north of the SSS maximum and SSS < 34.6), and

$$xCO_2s = 364.73 + 7.99 \cdot T_{25} + 12.56 \cdot S_{35} + 1.7 \cdot Yr_{2000} \quad (\pm 14.9) \qquad (2)$$

for Region F (southeastern subtropical region; south of the SSS maximum).
T_{25}, S_{35} and Yr_{2000} are [SST − 25], [SSS − 35] and [year − 2000], respectively. For the rest region (north of the SSS maximum and SSS ≥ 34.6) we used the same equation as that for Region D.

3.2.1.b. The South Pacific (SP/T)

Positive linear relationships were found between SST and xCO$_2$s in almost all regions of the subtropical South Pacific except for off Peru (Region J; green oval in Fig. 3d). The value for xCO$_2$s at SST = 25 °C from the linear regression gradually increases toward the east.

Off the coast of Peru, there is a negative linear relationship between SST and xCO$_2$s because of the influence of coastal upwelling (Region K; blue oval in Fig. 3d). This relationship is found only north of 20°S and east of 95°W from July to December. This region during this season is called the "coastal upwelling region". In contrast, there are no clear relationships between SSS and n-xCO$_2$s throughout the entire subtropical region (Fig. 3i).

We calculated a climatological linear regression equation for the relationship between SST and xCO$_2$s for each 1° × 1° grid by using the xCO$_2$s data corrected to the year 2000, and produced an empirical equation by adding the long term trend estimated in section 3.1 (1.7 ppm yr^{-1}) to this climatological equation for Region J:

$$xCO_2s = A(Lon, Lat) + B(Lat) \cdot T_{25} + 1.7 \cdot Yr_{2000} \qquad (3)$$

A and B are intercept and slope, respectively. Slope B is calculated for each 1° zonal band by using observational data between 170°E and 170°W. The intercept A is the xCO$_2$s at SST = 25 °C, corrected using the slope B.

In the coastal upwelling region, the linear relationship between SST and xCO$_2$s changes with latitude, because the upwelling strengthens toward the north. Therefore, we calculated a linear regression equation for each 1° zonal band in Region K:

$$xCO_2s = A'(Lat) + B'(Lat) \cdot T_{25} + 1.7 \cdot Yr_{2000} \qquad (4)$$

where A' and B' are intercept and slope, respectively.

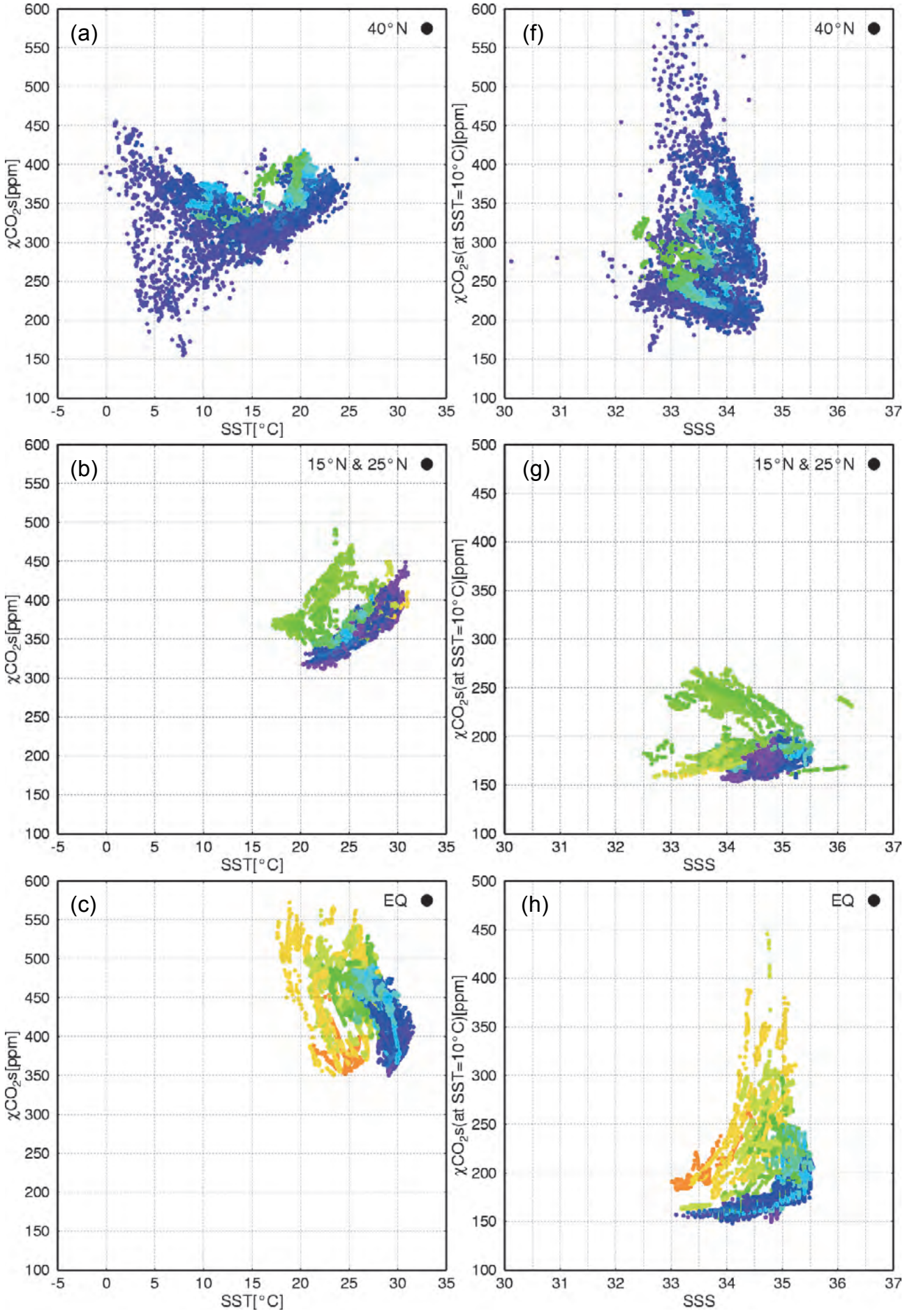
(a)
40°N
(b)
15°N & 25°N
(c)
EQ
(f)
40°N
(g)
15°N & 25°N
(h)
EQ
χCO2s[ppm]
χCO2s(at SST=10°C)[ppm]
SST[°C]
SSS

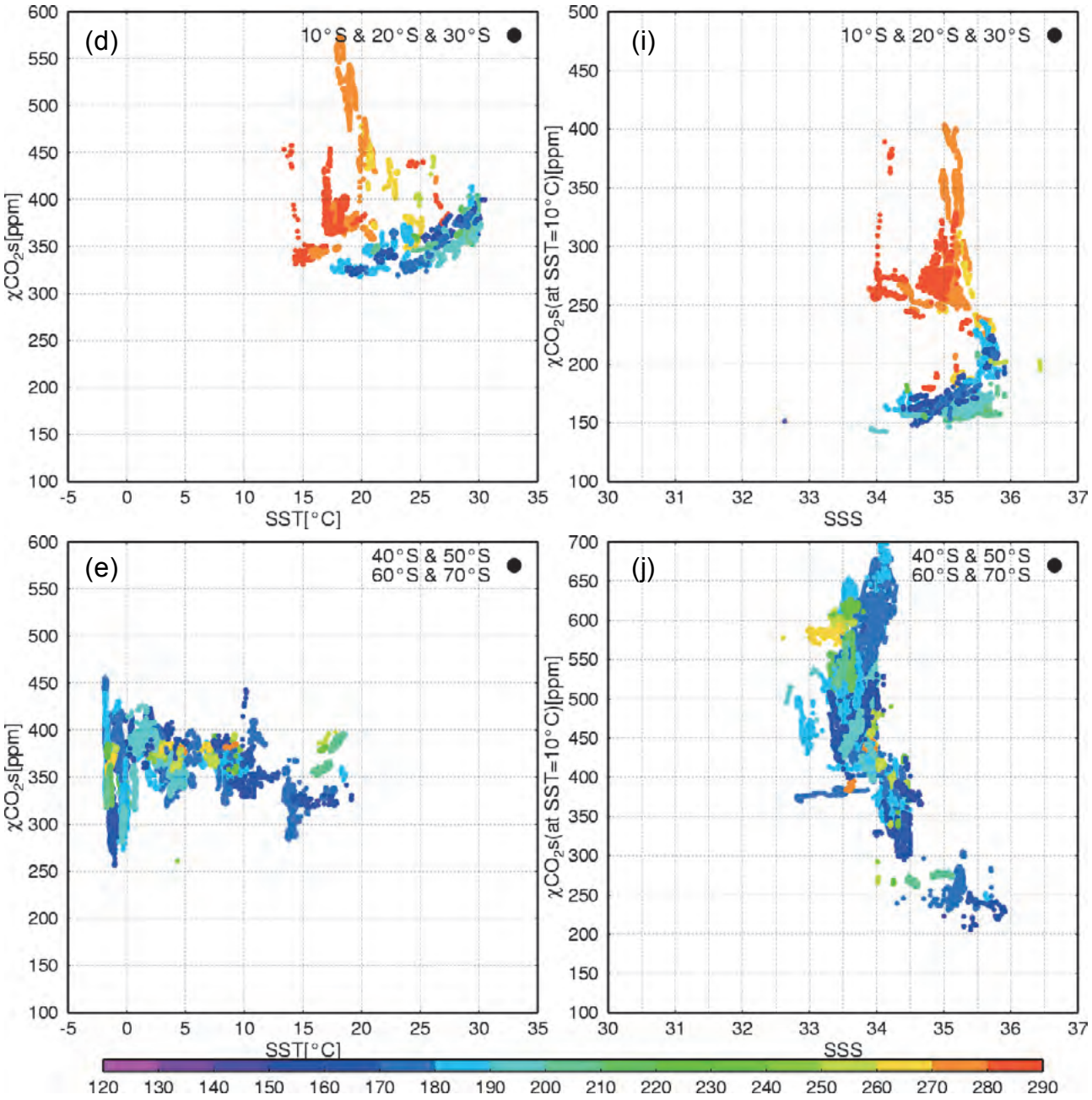

Figure 3. Relationships between xCO_2s and SST (left column) or SSS (right column) in five regions of the Pacific Ocean: (a) and (f), NP/A; (b) and (g), NP/T; (c) and (h), EQ; (d) and (i), SP/T; (e) and (j), SP/A. The labels “Positive” or “Negative” indicate the signs of the regression coefficients between xCO_2s and SST or SSS.

3.2.2. The equatorial region (EQ)

The easterly trade winds cause equatorial upwelling. This upwelling brings cold and carbon-rich water from deeper layers to the surface. In the equatorial region, SST and $x\mathrm{CO_2}$s are negatively correlated and this relationship varies seasonally and annually. Cosca et al. (2003) and Feely et al. (2006) used this relationship to derive seasonal and inter-annual equations for estimates of $p\mathrm{CO_2}$s. In contrast, Nakadate and Ishii (2007) and Ishii et al. (2009) used SSS to divide the equatorial region into the warm pool region and the upwelling region and derived two equations to calculate $x\mathrm{CO_2}$s. In this region ENSO determines the strength of upwelling and the wind patterns, which cause inter-annual variation of $\mathrm{CO_2}$ flux (Cosca et al., 2003; Feely et al., 2006; Nakadate and Ishii, 2007; Ishii et al., 2009).

In the equatorial upwelling region, we found a negative linear relationship between SST and $x\mathrm{CO_2}$s that varies seasonally, as reported by Cosca et al. (2003) and Feely et al. (2006) (blue oval in Fig. 3c). The relationship between SSS and n-$x\mathrm{CO_2}$s is a quadric convex distribution and n-$x\mathrm{CO_2}$s reaches a peak at SSS = 35 (blue oval in Fig. 3h).

The warm-pool region spreads to the west of the upwelling region where there is a positive linear relationship between SST and $x\mathrm{CO_2}$s. The relationship between SSS and n-$x\mathrm{CO_2}$s is not clear in this region (red oval in Fig. 3c and 3h). East of the upwelling region, SSS and $x\mathrm{CO_2}$s are relatively low (green oval in Fig. 3c and 3h). A positive relationship between SSS and n-$x\mathrm{CO_2}$s is seen in this region where SSS is above 34.

On the basis of these observations, we divided the equatorial region into three sub-regions: the warm pool region (G), the upwelling region (H) and the low salinity region (I). The geographic distribution of these three sub-regions varies with time depending on the distribution of SSS. The boundary between the upwelling region and the other two regions is defined by the following relationship:

$$SSS_{bnd} = \begin{cases} 35 & (\text{west of } 160^\circ\text{W}) \\ 35 + \dfrac{lon - 160}{40} & (\text{between } 160^\circ\text{W and } 120^\circ\text{W}) \\ 34 & (\text{east of } 120^\circ\text{W}) \end{cases} \qquad (5)$$

where '*lon*' indicates longitude in degrees west. The area where SSS $\geq SSS_{bnd}$ is classified as the upwelling region (Region H) and the region where SSS $< SSS_{bnd}$ contains the other two sub-regions. The area where SSS $< SSS_{bnd}$ is divided into two smaller regions at 140°W. The area west of 140°W is regarded as the warm pool region (Region G) and east of 140°W is the low salinity region (Region I).

Eq. 6 below is the empirical formula for the distribution of $x\mathrm{CO_2}$s in the equatorial region. We used a quadratic expression because of the quadric convex relationship between SSS and n-$x\mathrm{CO_2}$s in the upwelling region (blue oval in Fig. 3h). A sine-function term for the month ("*Mn*" in Eq. 6; 1 to 12 for January through December, respectively) is added to the equation only in the upwelling region to express the seasonal variation.

$$x\mathrm{CO_2s} = a + b \cdot T_{25} + c \cdot S_{35} + d \cdot {T_{25}}^2 + e \cdot {S_{35}}^2 + f \cdot T_{25} \cdot S_{35} + g \cdot Yr_{2000} + h \cdot \sin\left[2\pi \frac{Mn - i}{12}\right] \qquad (6)$$

The coefficients and root mean square errors (RMSEs) for each region are listed in Table 2.

Table 2. Coefficients and RMSEs for the multiple regression Eq. 5 for each sub-region in the equatorial Pacific (EQ). Letters after sub-region names correspond to the region codes in Figure 1.

Region	*a*	*b*	*c*	*d*	*e*	*f*	*g*	*h*	*i*	*RMSE* ppm
Warm pool (G)	455.76	-21.65	65.11	1.70	4.97	-8.18	1.97	—	—	12.6
Divergence area (H)	465.95	-10.51	9.29	-0.49	-66.86	2.86	1.31	14.87	0.40	27.4
Low salinity (I)	423.30	-1.23	53.56	0.65	8.51	-2.18	1.50	—	—	15.8

3.2.3. The subpolar regions

In the subpolar regions, strong vertical mixing supplies inorganic carbon from deep cold waters each winter. The increase in xCO_2s by vertical mixing exceeds xCO_2s reduction by seasonal cooling. There is a negative relationship between SST and xCO_2s in this region (Takahashi et al., 1993; Park et al., 2006).

In addition, phytoplankton consumes inorganic carbon in spring, with more consumption in the western North Pacific. To estimate the carbon reduction, previous studies have used Chl-*a* levels measured by remote sensing (Ono et al., 2004; Sarma et al., 2006; Chierici et al., 2009). In general, Chl-*a* is negatively correlated with xCO_2s because more carbon is consumed when more Chl-*a* is observed.

3.2.3.a The North Pacific (NP/A)

There is a positive linear relationship between SST and xCO_2s in the region of the subarctic North Pacific where SST ≥ 16 °C, as was also seen in the subtropical region (red oval in Fig. 3a). In this region, nutrients are exhausted and xCO_2s mainly varies from the thermodynamic effect. The intercept of the linear regression at 25 °C gradually increases toward the east. There is a negative relationship between SSS and n-xCO_2s in this region (red oval in Fig. 3f; referred as 'the northern subtropical region' (defined later)), with SSS increasing from west to east.

In the open ocean where SST < 16 °C and west of 160°E, there is a negative linear relationship between SST and xCO_2s (blue and orange ovals in Fig. 3a) and no significant relationship between SSS and n-xCO_2s.

In the region where 5 °C ≤ SST < 16 °C, the slope of the linear regression between SST and xCO_2s in summer (from July to September) is smaller than that in other seasons. This shows that the balance between factors that determine xCO_2s varies seasonally.

The slope of linear regression between SST and xCO_2s gets steeper in the region where SST < 5 °C because CO_2-rich water is supplied from deeper waters by the western subarctic circulation and vertical mixing.

In the Oyashio region and the region where SST < 16 °C, xCO_2s is very low and there is no clear relationship between SST and xCO_2s because phytoplankton blooms consume most of the CO_2 (green oval in Fig. 3a).

Based on these observations, we divided the subarctic region into three smaller regions: the northern subtropical region (SST ≥ 16 °C; Region C), the southern subarctic region (5 °C ≤ SST < 16 °C;

Region B) and the northern subarctic region (SST < 5 °C; Region A). We produced regression equations for each sub-region. Two equations are needed for the southern subarctic region to account for seasonal differences between summer and other seasons. The equation for Region A (SST < 5 °C) is as follows:

$$x\mathrm{CO}_2\mathrm{s} = 288.62 - 14.21 \cdot T_{10} + 1.40 \cdot Yr_{2000} \quad (\pm 24.6) \qquad (7).$$

The equation for Region B (Oct–Jun; 5 °C ≤ SST < 16 °C) is as follows:

$$x\mathrm{CO}_2\mathrm{s} = 345.42 - 3.10 \cdot T_{10} + 1.40 \cdot Yr_{2000} \quad (\pm 15.1) \qquad (8),$$

and for Jul–Sep (5 °C ≤ SST < 16 °C) as follows:

$$x\mathrm{CO}_2\mathrm{s} = 358.73 - 1.85 \cdot T_{10} + 1.40 \cdot Yr_{2000} \quad (\pm 21.2) \qquad (9).$$

For Region C (SST ≥ 16 °C), the equation is as follows:

$$x\mathrm{CO}_2\mathrm{s} = 248.10 + 9.86 \cdot T_{10} - 12.78 \cdot S_{33} + 0.76 \cdot Lon_{160} + 1.40 \cdot Yr_{2000} \quad (\pm 15.1) \qquad (10),$$

where T_{10}, S_{33}, Lon_{160} and Yr_{2000} are defined as [SST − 10], [SSS − 33], [longitude (°E) − 160] and [year − 2000], respectively.

It is also necessary to consider the biological activity in the regions off the Sanriku coast in Japan and around the Aleutian Islands (Ono et al., 2004; Sarma et al., 2006; Chierici et al., 2009). Chierici et al. (2009) reported that the use of log-transformed Chl-*a* data significantly improves the fit of the multiple regressions for estimating $p\mathrm{CO}_2$s.

We compared the logarithm of Chl-*a* with the residual error between estimated and observed $x\mathrm{CO}_2$s (Fig. 4a–4c) and found negative linear relationships. We generated linear regression equations to estimate the biological consumption of CO_2 (*Bio*) in each region.

Region A (SST < 5 °C): $Bio = -55.11 - 48.47 \cdot \ln[\mathrm{Chl\text{-}a}]$ (± 50.3) (11)

Region B (Oct–Jun ; 5 °C ≤ SST < 16 °C): $Bio = -44.85 - 36.27 \cdot \ln[\mathrm{Chl\text{-}a}]$ (± 29.3) (12)

Region B (Jul–Sep ; 5 °C ≤ SST < 16 °C): $Bio = -42.99 - 30.34 \cdot \ln[\mathrm{Chl\text{-}a}]$ (± 39.8) (13)

Negative values for *Bio* indicate that $x\mathrm{CO}_2$s is overestimated using SST and SSS and that CO_2 is consumed by biological activity. For the regions west of 160°E or north of 50°N only, where there is high biological activity, if Eq. 11–13 yield negative values for *Bio*, then the value for *Bio* is respectively added to $x\mathrm{CO}_2$s as estimated by Eq. 7–9. The introduction of the *Bio* term reduces the average bias of the estimates to ±10 ppm.

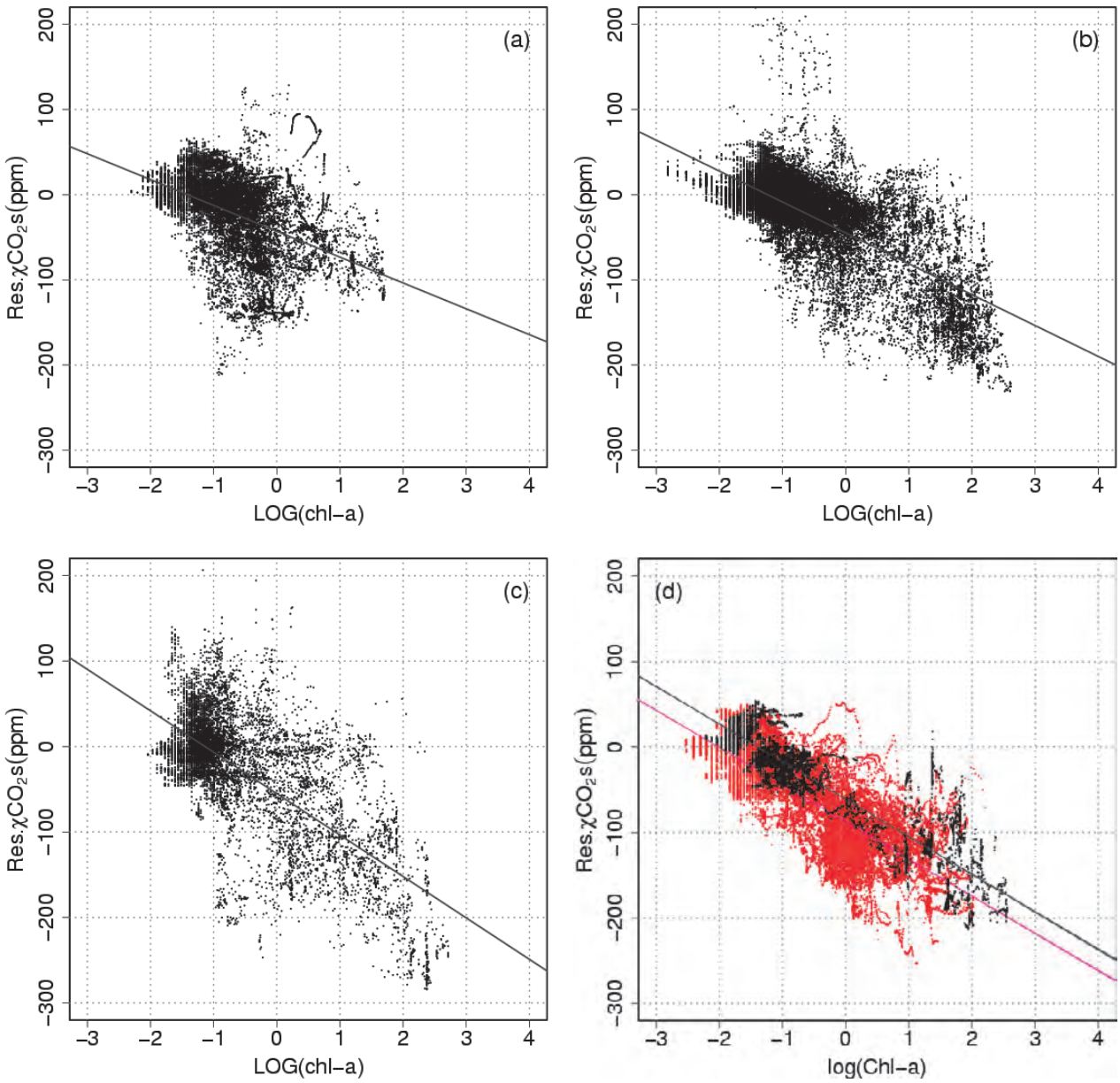

Figure 4. Relationships between the residual error between estimated and observed xCO_2s and the logarithm of chlorophyll-*a* concentrations determined by remote sensing from satellite. (a) The southern subarctic region within NP/A (summer: July–September), (b) the southern subarctic region within NP/A (winter: October–June), (c) the northern subarctic region within NP/A, (d) SST < 3℃ region within SP/A (black, October–December; red, January–April). Lines and shade areas are regression lines and 95% confidence intervals, respectively.

3.2.3.b. The South Pacific (SP/A)

The relationship between SST and xCO_2s changes at SST = 16 °C in the western portion of the South Pacific (140°E) and at SST = 10 °C in the east (70°W). This relationship is negative in the region of lower SSTs (orange oval in Fig. 3e) and positive at higher SSTs (red oval in Fig. 3e). In the region where SST < 3 °C, there is substantial biological consumption and no evident relationship between SST and xCO_2s when sea-ice melts in austral summer (green oval in Fig. 3e).

We divided the subantarctic South Pacific into three smaller regions using the following criteria:

1. Because the rates of increase of $x\mathrm{CO_2}$s differ between the northern region (north of 55°S) and the southern region (south of 55°S), as discussed in Section 3.1, the subantarctic South Pacific is divided into two regions at 55°S.
2. The northern region is divided into two regions by a boundary SST ($\mathrm{SST_{bnd}}$), defined as follows:

$$SST_{bnd} = 16 - \frac{6}{150}(longitude(°\mathrm{E}) - 140°\mathrm{E}) \qquad (14)$$

   The part of the northern region where SST < SST_{bnd} is called the northern subantarctic region (M) and where SST ≥ SST_{bnd} is the southern subtropical region (L).
3. The southern region (south of 55°S) is called the southern subantarctic region (N).

The relationship between SSS and n-$x\mathrm{CO_2}$s is negative in the southern subtropical region. We produced multiple regressions Eq. 15–17 to calculate $x\mathrm{CO_2}$s in the three regions using SST and SSS. For Region L (north of 55°S and SST ≥ $\mathrm{SST_{bnd}}$), the equation is as follows:

$$x\mathrm{CO_2s} = 322.90 + 2.23 \cdot T - 10.24 \cdot S_{33} + 0.44 \cdot Lon_{180} + 1.30 \cdot Yr_{2000} \quad (\pm 14.3) \qquad (15),$$

for Region M (north of 55°S and SST < $\mathrm{SST_{bnd}}$):

$$x\mathrm{CO_2s} = 399.97 - 6.62 \cdot T + 11.50 \cdot S_{33} + 1.30 \cdot Yr_{2000} \quad (\pm 15.0) \qquad (16),$$

and for Region N (south of 55°S):

$$x\mathrm{CO_2s} = 363.06 - 0.44 \cdot T + 4.19 \cdot S_{33} + 2.20 \cdot Yr_{2000} \quad (\pm 13.5) \qquad (17),$$

where Lon_{180} is the longitude (°E) minus 180.

In the Antarctic region (SST < 3°C), we introduce the *Bio* term to express biological consumption as in the subarctic region in the North Pacific. We produced two linear regression equations because the intercept of the regression between the logarithm of Chl-*a* concentration and the residual error of $x\mathrm{CO_2}$s from Eq. 17 changes between spring/early summer (October–December; black symbols in Fig. 4d) and late summer/autumn (January–April; red symbols in Fig. 4d). In areas where *Bio* was negative, as estimated by Eq. 18 and 19, it was added to $x\mathrm{CO_2}$s:

$$\text{Region N (Oct–Dec)}, \quad Bio = -61.05 - 43.94 \cdot \ln[\mathrm{Chl\text{-}a}] \quad (\pm 23.8) \qquad (18)$$

$$\text{Region N (Jan–Apr)}, \quad Bio = -87.56 - 43.49 \cdot \ln[\mathrm{Chl\text{-}a}] \quad (\pm 32.0) \qquad (19)$$